1-1-2014

Synergistic effect of self-assembled carbon nanopaper and multi-layered interface on shape memory nanocomposite for high speed electrical actuation

Haibao Lu

Fei Liang
University of Central Florida

Jihua "Jan" Gou
University of Central Florida

Wei Min Huang

Jinsong Leng

Synergistic effect of self-assembled carbon nanopaper and multi-layered interface on shape memory nanocomposite for high speed electrical actuation

Cite as: J. Appl. Phys. **115**, 064907 (2014); https://doi.org/10.1063/1.4865326
Submitted: 23 September 2013 . Accepted: 28 January 2014 . Published Online: 11 February 2014

Haibao Lu, Fei Liang, Jihua (Jan) Gou, Wei Min Huang, and Jinsong Leng

Synergistic effect of self-assembled carbon nanopaper and multi-layered interface on shape memory nanocomposite for high speed electrical actuation

Haibao Lu,[1,a)] Fei Liang,[2] Jihua (Jan) Gou,[2,b)] Wei Min Huang,[3] and Jinsong Leng[1,a)]
[1]*Science and Technology on Advanced Composites in Special Environments Laboratory, Harbin Institute of Technology, Harbin 150080, China*
[2]*Composite Materials and Structures Laboratory, Department of Mechanical, Materials and Aerospace Engineering, University of Central Florida, Orlando, Florida 32816, USA*
[3]*School of Mechanical and Aerospace Engineering, Nanyang Technological University, Singapore 639798, Singapore*

(Received 23 September 2013; accepted 28 January 2014; published online 11 February 2014)

The synergistic effect of self-assembled carbon nanofiber (CNF) nanopaper and the multi-layered interface on the electrical properties and electro-activated recovery behavior of shape memory polymer (SMP) nanocomposites is investigated. The CNFs were self-assembled by deposition into sheets of multi-layered nanopaper form to significantly enhance the bonding strength between the nanopaper and SMP via van der Waals force. The self-assembled multi-layered CNF nanopaper resulted in improved electrical conductivity and temperature distribution in the SMP nanocomposites. This not only significantly enhances the reliability of bonding between the nanopaper and the SMP, resulting in an improved recovery ratio, but also provides high speed electrical actuation. © *2014 AIP Publishing LLC*. [http://dx.doi.org/10.1063/1.4865326]

I. INTRODUCTION

Stimuli-responsive polymers are one of the many types of smart materials that could show noticeable changes in their properties continuously with the environmental conditions.[1,2] These responsive polymers can adapt to surrounding environments, in a number of ways including like altering colour or transparency, changing shape (shape memory polymers, SMPs), or converting electrical signals into optical, chemical, thermal and mechanical signals, and vice versa.[3–6] SMPs are able to change their shape or other chemical/physical properties in the presence of a particular stimulus.[7] The capability of shape switching may be utilized for motion generation, force generation or other functions.[8] If the deformed shape in a material can be virtually maintained forever, unless an appropriate external stimulus is applied as the driving force to trigger recovery back to the original shape, this phenomenon is defined as the shape memory effect (SME).[9] Unlike shape memory alloys (SMAs),[8] in which the reversible martensitic transformation between two crystalline phases is the underlying mechanism, the SME in SMPs functions via phase/state change resulting from molecular rearrangement and is predominantly an entropic phenomenon.[10–13] As one of the most popular actively moving materials, SMPs have many advantages, including low cost, light weight, a wide range of activation temperature (for heating-responsive shape recovery), high durability and high recoverable strain,[14–16] which currently attract great research interest. We have seen promising developments in many engineering applications, ranging from aerospace engineering to biomedical engineering.[17,18] Tremendous progress in synthesis, analysis, characterization, actuation technique and modeling now enable scientists to develop SMPs from a knowledge based approach.[19–22] Fundamental research aiming for alternative stimulation methods other than heating are still in high demand.[23–26] Among them, Joule heating to trigger the shape recovery is particularly of practical interest due to its convenience in implementation.[27] Electrically conductive SMP composites have been achieved by loading with various types of conductive fillers, such as carbon nanotubes (CNTs),[28] short carbon fibers,[29] carbon black,[30] carbon fiber,[31] carbon nanofibers (CNFs),[32] nanopaper,[33] graphene,[34] etc. Among these fillers, nanopaper shows some degree of success due to the significant improvement in electrical conductivity.[35] However, a large number of previous works were focused on conductive fillers blended into pure polymers. The resulting composites still could not achieve a high enough electrical conductivity to meet the requirements due to the limited efficiency of discrete fillers to form percolating conductive networks. A high loading level of filler is required, therefore, a high viscosity is produced due to strong interactions between the resin and the conductive filler, thus preventing an efficient transfer of the properties of the filler to the matrix. With regard to this challenge, we currently have introduced and explored nanopaper to the electrically conductive SMP nanocomposites.[34,35] However, the interface between the nanopaper and SMP composite could be damaged or even thermally degraded during heating due to the large dissimilarities in their thermally conductive properties. Consequently, the efficiency of heat transfer from the nanopaper to the underlying SMP composite is limited. SMP nanocomposites with multi-layered nanopaper are introduced in this work. The synergistic effect of self-assembled carbon nanofiber (CNF) nanopaper and multi-layered interface on the electrical property and electro-activated recovery behavior of SMP nanocomposites is reported. The CNFs were self-assembled by deposition into

[a)]Electronic address: luhb@hit.edu.cn and lengjinsong@hit.edu.cn.
[b)]Electronic mail: Jihua.Gou@ucf.edu.

multi-layered nanopaper to significantly enhance the bonding strength between nanopaper and SMP via van der Waals. The self-assembled multi-layered CNF nanopaper resulted in improved electrical conductivity and temperature distribution in the SMP nanocomposites. This not only significantly enhanced the reliability of the bonding between nanopaper and SMP resulting in an improved recovery ratio but also yielded high speed electrical actuation.

II. EXPERIMENTAL

CNFs were received in powder form with a nominal diameter ranging from 20 to 150 nm and length from 5 to 15 μm. The surfactant Triton X-100 of 2 ml was used to aid the dispersion of CNFs. The non-ionic surfactant (Triton X-100, $C_{14}H_{22}O(C_2H_4O)_n$) has a hydrophilic polyethylene oxide group and a hydrophobic group. The hydrophobic group of the surfactant backbone is in close contact with CNFs, resulting in the modified CNTs having a hydrophilic polyethylene oxide group. The raw CNFs of 0.6 g were mixed with 600 ml of distilled water to form a suspension. The CNF suspension was then sonicated with a high-intensity sonicator at 22 °C for 20 min at an ultrasound power level of 1200 W. The CNF suspension was membrane filtrated step by step under a positive pressure (with a gradient increase to control the interfacial bonding of CNFs) in order to self-assemble into sheets of nanopaper form with the aid of a hydrophilic polycarbonate membrane (with a diameter of 55 mm and 0.4 μm in gap). Each sheet in nanopaper could be therefore separated from each other by the resin transfer molding technique. After filtration, the CNF nanopaper was dried in an oven at 120 °C for 2 h to further remove the remaining water and surfactant.

The SMP used in the course of this study was a polyurethane-based fully formable thermoset SMP resin, with a glass transition temperature (T_g) of 50 °C. A resin transfer molding technique was applied to make SMP nanocomposites, as shown in Fig. 1. In the fabrication process, the one-layered, two-layered, three-layered, and four-layered nanopapers were first, respectively, placed on the bottom of the metallic mold. An amount of thermosetting polyurethane-based shape memory resin was inserted before the molding takes place. And a plunger was used to force the shape memory resin from the pot through channels into the mold cavities. After filling the mold, the mold was closed and remained in compression molding under hydraulic pressure of 6 bar. Finally, the thermosetting polyurethane-based shape memory resin was cured at 22 °C in a vacuum for 24 h, to produce the final SMP nanocomposites.

III. RESULTS AND DISCUSSION

A. Morphology and structure

The morphology and structure of the SMP nanocomposite were characterized using field emission scanning electron microscopy (FESEM, Zeiss Ultra-55). Fig. 2(a) shows a typical cross section of an SMP nanocomposite incorporated with self-assembled two-layered CNF nanopaper. The areas of nanopaper (dark phase) are distinct from the SMP matrix (lighter phase), indicating that there is interfacial bonding between the two phases. Multi-layered interface of the nanopaper is expected to significantly improve the interface bonding in SMP nanocomposites. Fig. 2(b) reveals the morphology and structure of the interface between the multi-layered nanopaper and SMP matrix at two scales. It is shown that the polymer resin is evenly impregnated throughout the nanopaper at the interface.

B. Electrical resistivity measurement

The bulk (volume) resistivity of the multi-layered nanopaper and SMP nanocomposite was characterized by a four-point probe apparatus (SIGNATONE QUAD PRO computerized four point resistivity system). The apparatus contains four thin collinearly placed tungsten wires probes which are made to contact the sample being tested. The electrical resistivity of the nanopapers with different layers is plotted against different measurement times in Fig. 3(a). Each data point denotes the average resistivity at different measurement times of 1, 5, 9, and 13, respectively. Standard deviation is also indicated. As we can see, with the increase in the number of layers of nanopaper, the electrical resistivity of the resultant composite decreased from 6.8 Ω·cm to 1.6 Ω·cm. This is because more conductive paths are formed in a composite with more layers of nanopaper. Therefore, the electrical resistivity is reduced accordingly.[36] The electrical resistivities of nanopapers and their nanocomposites as a function of the number of layers of CNF nanopaper are presented in Fig. 3(b). All volume concentration of nanopaper within each nanocomposite is 10 vol. %, while the thicknesses of the one-, two-, three-, and four-layered nanopaper are 0.1 mm, 0.2 mm, 0.3 mm, and 0.4 mm, respectively. Correspondingly, the thicknesses of the nanocomposites are 1 mm, 2 mm, 3 mm, and 4 mm, respectively. We can see

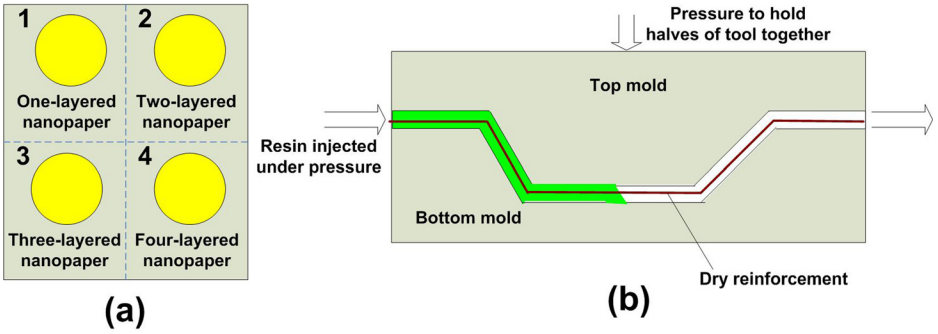

FIG. 1. The illustration of resin transfer molding process in the fabrication of SMP nanocomposite. (a) Nanopaper was first placed onto the bottom of the metallic mold (the locations were marked in yellow color). (b) Shape memory resin was transferred into the mold.

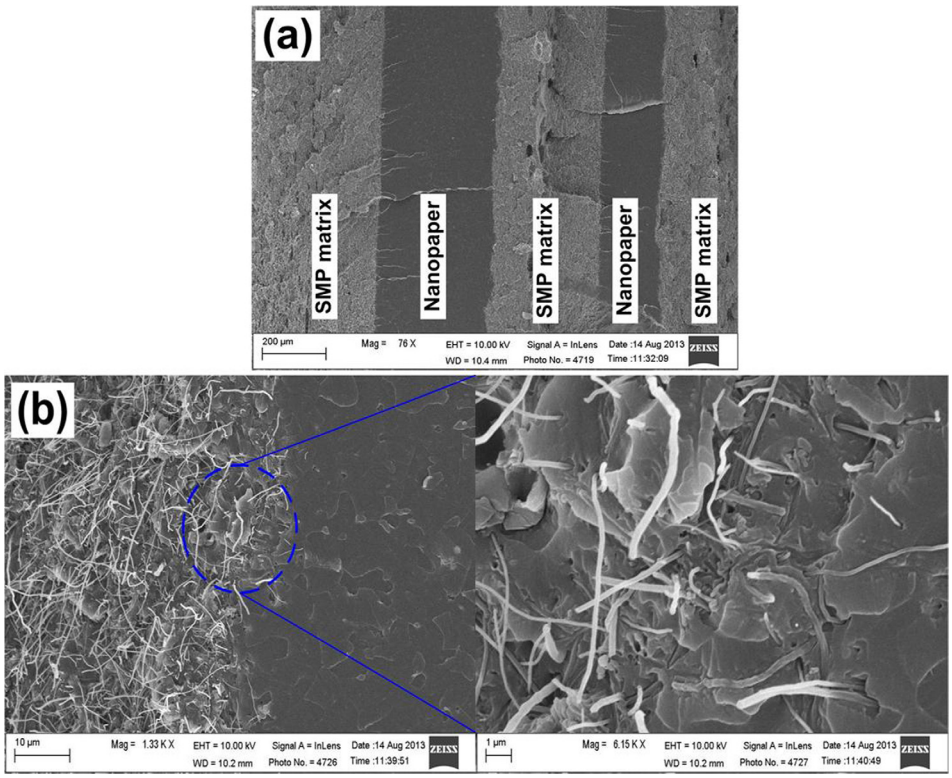

FIG. 2. (a). Morphology and structure of multi-layered nanopaper enabled SMP nanocomposite. (b). Morphology and structure of the interface between the multi-layered nanopaper and SMP matrix.

from these two curves that the electrical resistivity of the nanocomposite is always lower than that of the corresponding nanopaper. The interaction between the polymer and nanopaper should be the reason. The nanopaper is actually a porous structure. The polymer resin penetrates into or even through the CNFs in the interface. The density of nanopaper is altered as the bonding among the CNFs with the nanopaper changed from the van der Waals force to chemical linking provided by the polymer. Consequently, the electrical resistivity of the nanopaper is improved.

C. Electrically triggered shape recovery behavior

To demonstrate the synergistic effect of self-assembled carbon nanopaper and a multi-layered interface on electrical actuation, two "∏" shaped SMP nanocomposite samples (with two-layered and four-layered nanopaper, respectively) with dimensions of $80 \times 10 \times 2$ mm^3 and $80 \times 10 \times 4$ mm^3 were prepared for comparative testing. The samples were pre-bent into a "U" shape (temporary shape) at 80 °C. This temporary shape was maintained until the sample was cooled down to room temperature. No apparent shape recovery was observed after the deformed sample was kept in the air for 30 min. Subsequently, a 30 V DC voltage was applied, and an infrared video camera (FLIR Infrared Camera) was used to monitor the temperature distribution and shape recovery simultaneously. Snapshots of shape recovery sequence of both samples were shown in Fig. 4. Due to the reduction in electrical resistivity, the heating efficiency of the SMP nanocomposite with four-layered nanopaper was higher. Within

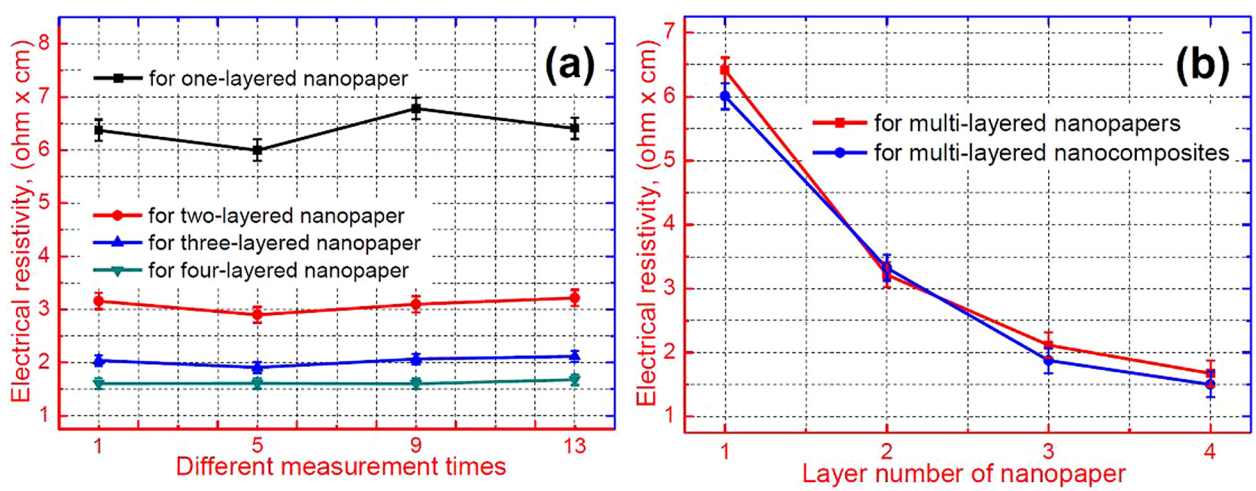

FIG. 3. (a). Electrical resistivity of one-, two, three-, and four-layered CNF nanopapers, each experimental data was measured one, five, nine and thirteen times, respectively. (b). Electrical resistivity curves of the multi-layered nanopapers and their SMP nanocomposites.

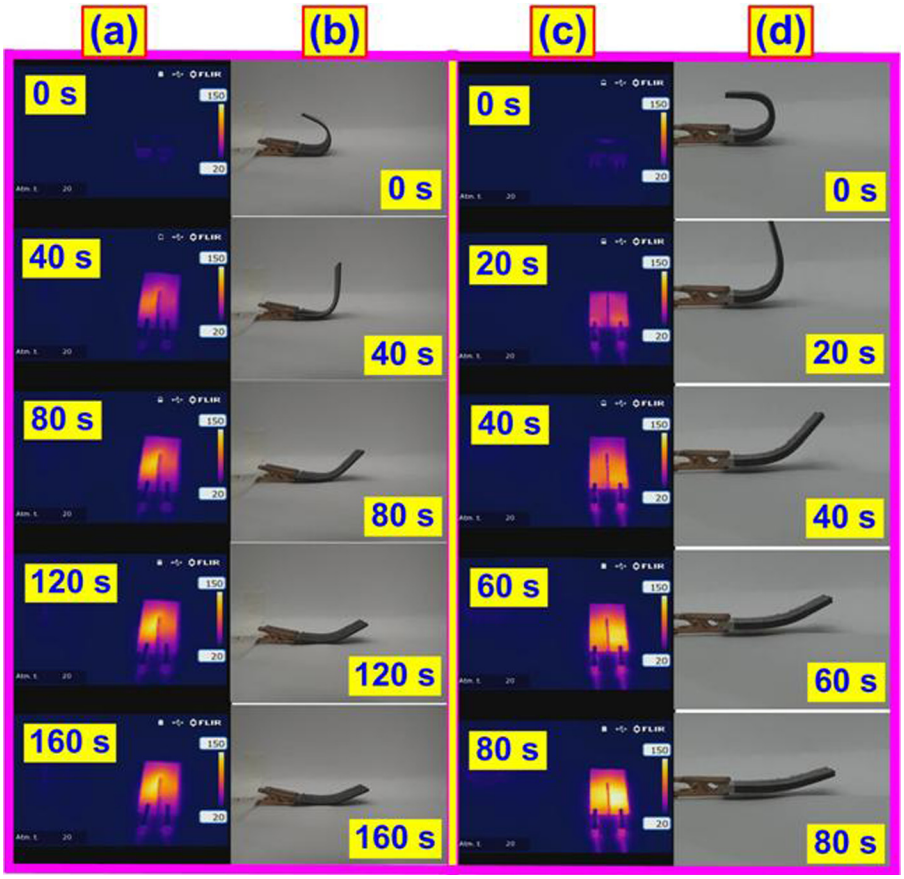

FIG. 4. Sequence of temperature distribution and shape recovery. (a). Temperature distribution of SMP nanocomposite incorporated with two-layered CNF nanopaper. (b). Shape recovery of SMP nanocomposite incorporated with two-layered CNF nanopaper. (c). Temperature distribution of SMP nanocomposite incorporated with four-layered CNF nanopaper. (d). Shape recovery of SMP nanocomposite incorporated with four-layered CNF nanopaper.

80 s, the nanocomposite sample with four-layered nanopaper was heated above 100 °C, and a full shape recovery was achieved. The power consumption of the sample was about 15 W and 0.5 A. For comparison, an SMP nanocomposite with two-layered CNF nanopaper took 160 s to regain the original flat shape at the same electric voltage. However, the two-layered nanopaper enabled SMP nanocomposite reached a temperature of about 80 °C at 80 s, with a power consumption of 6.9 W. Furthermore, temperature distributions in both samples are plotted in Fig. 5. In this manner, the temperature distribution and shape recovery process were simultaneously recorded and monitored for the electrical actuation of the SMP nanocomposite. High temperatures were found in the deformed locations where internal strains were higher than the others of the tested SMP nanocomposite. With electricity being applied, Joule heating resulted in a gradually increasing temperature. At 80 s, the maximum temperature of the two-layered nanopaper enabled SMP nanocomposite reached approximately 120 °C, while that of the four-layered nanopaper enabled SMP nanocomposite was 102.5 °C. On the other hand, the temperature distribution occurred within a temperature range from 53 to 120 °C and 83 to 105 °C for the two-layered and four-layered nanocomposites, respectively. Uniform temperature distribution is identified as the reason behind the excellent recovery behavior (fast recovery time, high recovery ratio, and anti-thermal degradation) of the electro-activated SMP nanocomposite. It was found that the synergistic effect of temperature range and temperature distribution on the electrical actuation of SMP nanocomposites plays a critical role in determining their recovery performance.

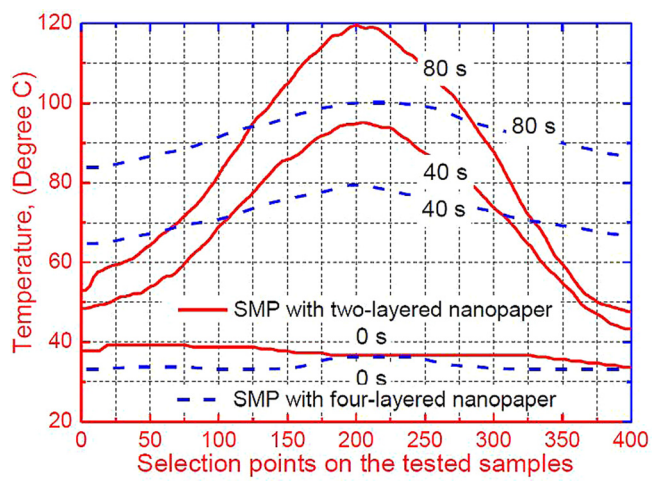

FIG. 5. Temperature distribution curves of the two-layered and four-layered SMP nanocomposites driven by loading an electric voltage of 30 V at various heating times of 0 s, 40 s, and 80 s, respectively.

Furthermore, each image was analyzed to determine the deformation angle, where the initial deformation angle of the fixed sample shown in the first image is considered as θ_e (in our case $\theta_e = 0$). The recovery ratio, R, is defined as,[37]

$$R(\%) = \frac{\theta_i - \theta(t)}{\theta_i - \theta_e}, \quad (1)$$

where $\theta(t)$ and θ_i are the deformation angle at a given time t and the deformation angle at the equilibrium state, respectively. The recovery experiments were carried out under

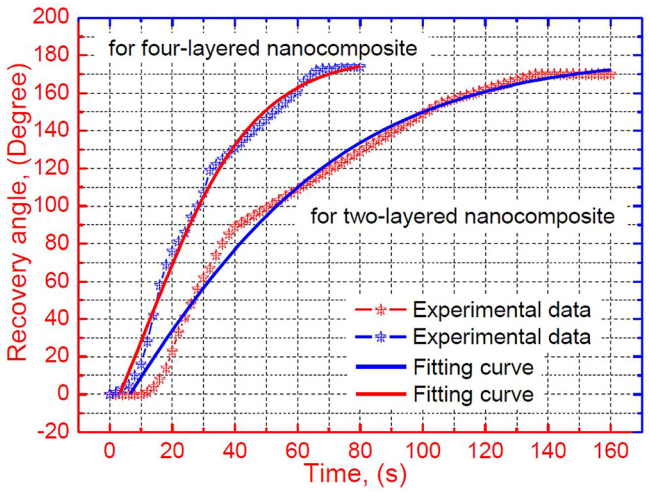

FIG. 6. Time-resolved photographs of electrically activated shape recovery of SMP nanocomposites. Four-layered nanopaper enabled nanocomposites showing faster recovery than that with two-layered nanopaper under a constant DC voltage of 30 V.

30 V DC voltage and the resulting recovery profiles are presented in Fig. 6. It is shown that the four-layered nanopaper enabled SMP nanocomposite revealed dramatically faster recovery than that with two-layered nanopaper. Therefore, the additional multi-layered nanopaper can indeed significantly accelerate the recovery time of the SMP matrix.

To reveal more detailed kinetic information for the recovery behavior of the tested samples, the recovery data were further analyzed using a standard Boltzmann (sigmoidal) function:

$$R(t) = A_2 + \frac{A_1 - A_2}{1 + e^{(x - x_0)/dx}}, \tag{2}$$

where A_1, A_2, t_0, and τ are the four fitting parameters. All four fitting parameters can be obtained from the experimental results. So, the dataset for each curve is "$A_1 = -298.55$, $A_2 = 180.10$, $x_0 = -15.093$ and $dx = 42.617$" and "$A_1 = -110.13$, $A_2 = 179.67$, $x_0 = 11.553$ and $dx = 17.366$," respectively. The fit curves had respective R^2 values of 0.98854 and 0.99264, and are shown as solid lines. It was found that the recovery time of the SMP nanocomposite with four-layered CNF nanopaper (at 96.7% in recovery ratio) was 80 s shorter than that with two-layered CNF nanopaper (at 94.4% in recovery ratio) under the 30 V triggering voltage. This fact can be attributed to the multi-layered nanopaper that facilitates the heat transfer from the nanopaper to the underlying SMP. This significantly enhances heat transfer and yields high speed electrical actuation.

As shown in Fig. 7(a), the SMP nanocomposite specimen incorporated with four-layered CNF nanopaper had the fastest response (it returned to the permanent shape within 80 s) to the electrical stimulus. Furthermore, it presented the highest recovery ratio of approximately 96.7%. On the other hand, the nanocomposite with one-layered nanopaper had the slowest response (it returned to the permanent shape within 197 s), and the recovery ratio was approximately 92.8%. Therefore, the content of nanopaper in the SMP nanocomposite had a positive effect on the shape recovery speed and shape recovery ratio. When the nanocomposite was incorporated with four-layered nanopaper, it had an 80 to 85 s response time to the electrical stimulus. Furthermore, there was little loss in recovery ratio after the cyclic recovery was repeated up to 5 times, as shown in Fig. 7(b). However, the one-layered nanopaper enabled nanocomposite had a 197 to 241 s response time to the electrical stimulus. The loss in recovery ratio goes from bad to worse after the cyclic recovery is repeated up to 5 times. Therefore, the positive role of the multi-layer in SMP resin is presented, i.e., fast electrically responsive behavior and excellent recovery ratio. The relative motion of macromolecule segments or chains is the primary mechanism of the SME in SMP. During the process of shape recovery, the packed macromolecular segments must overcome external constraints to return to the permanent shape. CNFs could reinforce the polymer matrix and improve the recovery strength to help the SMP to return to its original configuration.[38] The macromolecule segments in nanocomposites have high recovery force in comparison to that of pure SMP. With an increase in the content of nanopaper, more CNFs are involved to reinforce the polymer matrix

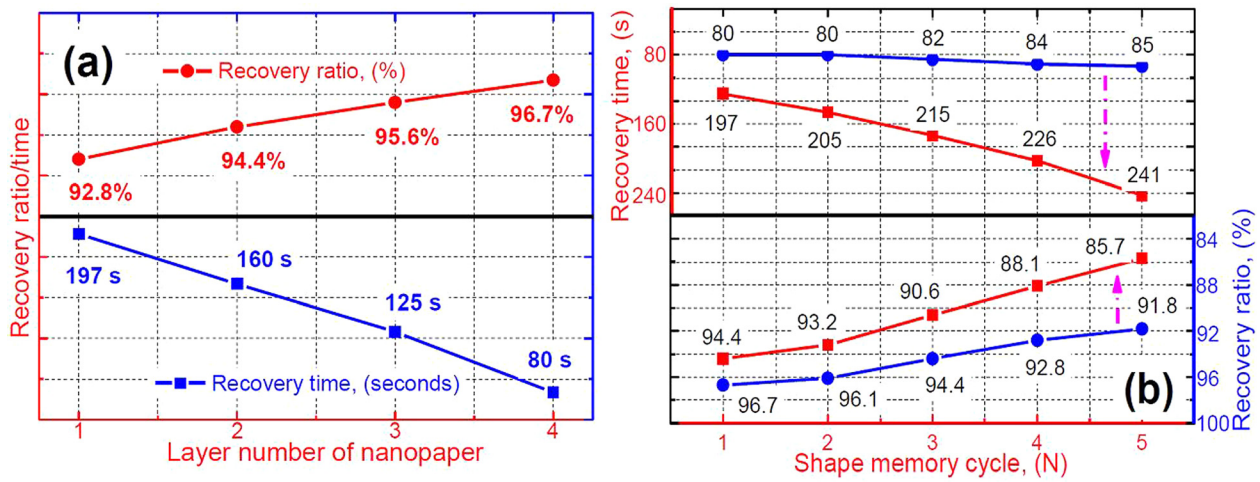

FIG. 7. (a) Comparison in recovery behavior of SMP nanocomposites incorporated with one-, two-, three-, and four-layered nanopaper. (b) Comparison in recovery behavior of SMP nanocomposites incorporated with two- and four-layered nanopaper as a function of shape memory cycle.

due to the increased interfaces between the SMP and nanopaper. Therefore, the four-layered nanopaper enabled SMP nanocomposite had the highest recovery ratio, relatively. Furthermore, these CNF nanopapers could significantly improve the electrical and thermal conductivities to facilitate the heat transfer from the nanopaper to the SMP part. Therefore, the speed of electro-activated response is also significantly increased in the SMP nanocomposite incorporated with four-layered nanopaper. It should be noted that the thickness should be another important factor. For a given bending curvature, the compressive and tensile strains on the top and bottom surface of the thicker beam are much higher than the thinner beam. The higher strain energy stored in the thicker actuator could also attribute to the fast recovery speed.

IV. CONCLUSIONS

A series of experiments were conducted to study self-assembled carbon nanopapers and the effect of their multi-layered interfaces on shape-memory nanocomposites. The CNFs were self-assembled into multi-layered nanopaper to significantly enhance the electrical properties and reliability in bonding between the nanopaper and SMP matrix. The actuation of the SMP nanocomposites was achieved by the electrically resistive heating of multi-layered CNF nanopaper that facilitated the heat transfer from the nanopaper to the underlying SMP. This not only improved electrical conductivity and heat transfer but also provided high speed electrical actuation.

[1]S. H. Low, L. L. Shiau, and G. K. Lau, Appl. Phys. Lett. **100**, 182901 (2012).
[2]P. J. Cottinet, C. Souders, S. Y. Tsai, R. Liang, B. Wang, and C. Zhang, Phys. Lett. A **376**, 1132–1136 (2012).
[3]J. E. Martin and R. A. Anderson, J. Chem. Phys. **111**, 4273 (1999).
[4]M. Moscardo, X. H. Zhao, Z. G. Suo, and Y. Lapusta, J. Appl. Phys. **104**, 093503 (2008).
[5]D. Guyomar, K. Yuse, P. J. Cottinet, M. Kanda, and L. Lebrun, J. Appl. Phys. **108**, 114910 (2010).
[6]P. J. Cottinet, M. Q. Le, J. Degraff, C. Shouders, Z. Liang, B. Wang, and C. Zhang, Sens. Actuators A **194**, 252–258 (2013).
[7]A. Lendlein and S. Kelch, Angew. Chem. Int. Ed. **41**, 2034–2057 (2002).
[8]L. Sun, W. M. Huang, Z. Ding, Y. Zhao, C. C. Wang, H. Purnawali, and C. Tang, Mater. Des. **33**, 577–640 (2012).
[9]C. Liu, H. Qin, and P. T. Mather, J. Mater. Chem. **17**, 1543–1558 (2007).
[10]B. A. Nelson, W. P. King, and K. Gall, Appl. Phys. Lett. **86**, 103108 (2005).
[11]I. A. Rousseau, Polym. Eng. Sci. **48**, 2075–2089 (2008).
[12]L. Sun and W. M. Huang, Soft Matter **6**, 4403–4406 (2010).
[13]T. Xie, Polymer **52**, 4985–5000 (2011).
[14]K. Gall, M. L. Dunn, Y. P. Liu, and G. Stefanic, Appl. Phys. Lett. **85**, 290–292 (2004).
[15]I. Gurevitch and M. S. Silverstein, Soft Matter **8**, 10378–10387 (2012).
[16]J. S. Leng, H. B. Lv, Y. J. Liu, and S. Y. Du, Appl. Phys. Lett. **91**, 144105 (2007).
[17]D. J. Maitland, M. F. Metzger, D. Schumann, and A. Lee, Laser. Surg. Med. **30**, 1–11 (2002).
[18]P. R. Buckley, G. H. McKinley, T. S. Wilson, W. Small, W. J. Benett, J. P. Bearinger, M. W. McElfresh, and D. J. Maitland, IEEE Trans. Biomed. Eng. **53**, 2075–2083 (2006).
[19]P. T. Mather, X. F. Luo, and I. A. Rousseau, Annu. Rev. Mater. Res. **39**, 445–471 (2009).
[20]H. B. Lu, W. M. Huang, and Y. T. Yao, Pigm. Resin Technol. **42**, 237–246 (2013).
[21]M. Behl, J. Zotzmann, and A. Lendlein, Adv. Polym. Sci. **226**, 1–40 (2010).
[22]J. L. Hu, Y. Zhu, H. H. Huang, and J. Lu, Prog. Polym. Sci. **37**, 1720–1763 (2012).
[23]H. Koerner, G. Price, N. A. Pearce, M. Alexander, and R. A. Vaia, Nature Mater. **3**, 115–120 (2004).
[24]W. M. Huang, B. Yang, L. An, C. Li, and Y. S. Chan, Appl. Phys. Lett. **86**, 114105 (2005).
[25]R. Mohr, K. Kratz, T. Weigel, M. Lucka-Gabor, M. Moneke, and A. Lendlein, Proc. Natl. Acad. Sci. U.S.A. **103**, 3540–3545 (2006).
[26]G. Li, G. Fei, H. Xia, J. Han, and Y. Zhao, J. Mater. Chem. **22**, 7692–7696 (2012).
[27]J. S. Leng, H. B. Lv, Y. J. Liu, and S. Y. Du, J. Appl. Phys. **104**, 104917 (2008).
[28]H. H. Le, O. Osazuwa, I. Kolesov, S. Ilisch, and H. J. Radusch, Polym. Eng. Sci. **51**, 500–508 (2011).
[29]H. H. Le, A. Zulfiqar, U. Mathias, S. Ilisch, and H. J. Radusch, J. Appl. Polym. Sci. **120**, 2138–2145 (2011).
[30]H. B. Lu, Y. T. Yao, and L. Lin, Pigm. Resin Technol. **43**, 26–34 (2014).
[31]X. Lan, Y. J. Liu, H. B. Lv, X. H. Wang, J. S. Leng, and S. Y. Du, Smart Mater. Struct. **18**, 024002 (2009).
[32]I. S. Gunes, G. A. Jimenez, and S. C. Jana, Carbon **47**, 981–997 (2009).
[33]Z. Tang, D. Sun, D. Yang, B. Guo, L. Zhang, and D. Jia, Compos. Sci. Technol. **75**, 15–21 (2013).
[34]H. B. Lu, F. Liang, and J. Gou, Soft Matter **7**, 7416–7423 (2011).
[35]H. B. Lu and J. H. Gou, Nanosci. Nanotech. Lett. **4**, 1155–1159 (2012).
[36]H. B. Lu, Y. J. Liu, J. H. Gou, J. S. Leng, and S. Y. Du, Smart Mater. Struct. **19**, 075021 (2010).
[37]X. F. Luo and P. T. Mather, Soft Matter **6**, 2146–2149 (2010).
[38]G. A. Jimenez and S. C. Jana, Polym. Eng. Sci. **49**, 2020–2030 (2009).